



Fermi National Accelerator Laboratory

FERMILAB-TM-1935

Testing of the Scintillation Sandwich Prototype

Dr. Vyacheslov Vashkevich

*Institute of Nuclear Physics
Moscow State University*

*Fermi National Accelerator Laboratory
P.O. Box 500, Batavia, Illinois 60510*

June 1995

Disclaimer

This report was prepared as an account of work sponsored by an agency of the United States Government. Neither the United States Government nor any agency thereof, nor any of their employees, makes any warranty, express or implied, or assumes any legal liability or responsibility for the accuracy, completeness, or usefulness of any information, apparatus, product, or process disclosed, or represents that its use would not infringe privately owned rights. Reference herein to any specific commercial product, process, or service by trade name, trademark, manufacturer, or otherwise, does not necessarily constitute or imply its endorsement, recommendation, or favoring by the United States Government or any agency thereof. The views and opinions of authors expressed herein do not necessarily state or reflect those of the United States Government or any agency thereof.

Testing of the Scintillation Sandwich Prototype

Dr. Vyacheslov Vashkevich
Institute of Nuclear Physics
Moscow State University

The 3 m² area prototype of the surface detector using optical fiber readout was completely prepared for testing measurements in February 1995 at Fermilab. The configuration of the detector is described in detail in ¹. Two 25 mm thick, 3 m² acrylic scintillation plates (1.2 x 2.5 m²) are used for light collection in the upper (above the 25 mm steel plate) and lower (below the steel) counters of the sandwich (Fig. 1). The light is collected with the help of 1 mm diameter wavelength shifter fiber loops 3 m long inserted in the grooves on the top surface of the scintillator, 3 fibers per groove. We used Kuraray Y11, 200 ppm of shifter dye, and double clad fibers. 1.5 m of clear fibers spliced to each end of the shifter fiber transport the light to the phototube. Spacing between the grooves is 5 cm. The counter's edges were painted with BICRON (BC620) white reflective paint. The scintillation plates were wrapped with Dupont Tyvek. The glued bundle of fibers is connected to an EMI-9902KB 38 mm phototube through the simple light mixer bar. Used PM has a "green extended" rubidium bialkali photocathode.

The light yield of counters of this type for different groove spacing, groove depth and number of fibers per groove was studied in the above mentioned work of Paul Mantsch et al. It was shown that the light yield is practically insensitive to both the depth of the fiber in the groove and the groove's depths of 5 mm and 10 mm. Decreasing the spacing between the grooves by the factor 2 adds about 35% in light yield. It was also shown that each additional fiber adds about 50% of the light of the first fiber in the groove.

Fig. 2a represents the typical pulse-height distribution of the muon's signals measured for the upper 3 m² counter by charge ADC driven by coincidence signals of the upper and lower counters. To characterize a pulse-height distribution we use the truncated mean and sigma values that determined as mean and sigma of the portion of the distribution between 20 and 200% of the truncated mean.

The direct spectrum without any coincidences is presented on Fig. 2b. One can see that the light yield and the areal uniformity in our simple flat detector of 3 m² area with one small fast phototube are high enough to separate one particle peak in pulse-height spectrum from the noise signals without the selection of cosmic ray muons with the help of coincidences with additional counters. This is one of the advantages in comparison with the classical method when the scintillator is viewed with the big PM tube in a large cone or pyramid through the air or in comparison with the counters using wavelength shifter bars.

Calibration of the phototube with the single photoelectron peak measurements was made and it was shown that the mean number of

photoelectrons produced by the light flash in our counter is about 23 (Fig. 3). This fact allows us to achieve the high efficiency of the registration of single particles (>95%) without the significant decreasing of the discriminator threshold that corresponds to the increase of the counting rate and the high deposit of noise signals after the discriminator. The dependence of the registration efficiency for the upper and lower counters of the sandwich prototype on the counting rate (changed with the discriminator's threshold) is presented on Fig. 4. The single rates corresponding to 95% of the registration efficiency are found to be equal to 800 and 1100 per sec for the upper and lower counters respectively (the lower counter is slightly more noisy).

The high areal uniformity of the sandwich prototype was demonstrated for both counters during the testing measurements with the help of a telescope consisting of two 15x15 cm² small scintillation counters (see ¹ and Fig. 5). The maximum difference in light yield over the 3 m² area is less than 30%. This difference is due mainly to the decrease in thickness of the scintillation plates from the edges to the center.

Some main time characteristics of the sandwich prototype were obtained during the primary testing. The dead time of the counters, the time resolution of the detector, and the coincidence window that we should use to register the "top-bottom" coincidences with high efficiency were estimated. We should also estimate the influence of re-triggerings of the PM pulse discriminator and afterpulses of the phototube.

The dependence of the truncated mean in pulse-height distribution of the anode's signals vs. duration of the gates for charge ADC is presented on Fig. 6. The gates required to capture >90% of the charge are less than 100 ns. Using this dependence we can estimate the average fall time of the anode signal. The derivative of this curve reflects the change of the charge deposit with time. The characteristic fall time of this exponential tail is about 20 ns. The average pulse duration on the level of 1/10 of amplitude is about 60 ns and the duration of the mean signal with the ideal average shape on the threshold level corresponding to 95% of registration efficiency is about 30 ns (Fig. 7). These values characterize the decay time of the wavelength shifter in the readout fibers.

However, these estimations are made for the ideal average signals. The real signal has more complicated form with the fluctuations of the charge deposit in time and the complex tail (see Fig. 8a, 8b, 8c). So we need to estimate the influence of these fluctuations that can produce the aftertriggering signals. It is also necessary to estimate the influence of the afterpulses of the phototube.

To look for two correlated pulses the LeCroy CAMAC TDC-4208 unit operating in multi-hit mode was used. It can measure the time intervals between as many as 8 sequential signals coming to one input. The time resolution of this TDC is 1 ns. It required two pulses within 2 microseconds

and measured the time difference between these pulses. The minimum duration of the discriminator's signals was established to be equal to 100 ns and the threshold level corresponded to 95% of registration efficiency. The distribution of time intervals between 2 signals from the discriminator of anode pulses for the upper counter was measured (see Fig. 9). According to Poisson distribution for independent signals, this distribution must be uniform in a short interval that is much less than the mean period of the signal's sequence (~1 ms). The experimental distribution has two weak peaks, each amounting to less than 0.5% of the singles rate. The first peak is caused by the low amplitude fluctuations of the signal's tail after 100 ns. It was shown that a little increasing of the discriminator's threshold to the level corresponding to 90% of registration efficiency removes the first peak almost completely (Fig. 9a). The second peak at about 500 ns is due to the afterpulsing of the phototube. It was demonstrated in the experiment with a light emitting diode illuminating the tested PM (see copy of the scope screen, Fig. 9b). The same distribution was obtained for the lower counter and for "top-bottom" coincidences (in the last case the first peak amount <0.03% of the single coincidences rate and the second <0.01%) (Fig. 10). Therefore both of the effects can be neglected taking into account the Station alert conditions (4 particles in 10 m² station).

The time resolution of the counters in the scintillation sandwich (the accuracy of the arrival time determination) was determined with the help of the used TDC operating in single hit mode. The fluctuations of time delay between the signals from the discriminators of the upper and lower counters when a cosmic ray's muon penetrates both the plates is connected with this characteristic of the scintillation detector. The results of the measurements are presented on Fig. 11. Using this distribution we can determine the duration of the coincidence window that we should establish to register 98% of real "top-bottom" coincidences (see Fig. 12). A window of 28 ns gives this level of efficiency.

Summarizing the presented simple estimations we can conclude that the obtained results satisfy the performance requirements for surface detector to the Giant Airshower Detector ². See also the table below.

¹ P. Mantsch, S. Gourlay, J. Ozelis. A Large Area Air Shower Detector Using Optical Fiber Readout. January 1995.

² The Detection of 10²⁰ eV Cosmic Rays (The CYCLOPS/P5000 Project). January 1995.

Note 4

Trigger Condition

Composition sensitivity

Muon identification >90%, 1km, 10**20eV Note 2

Electron identification >90%, 1km, 10**20eV Note 2

Photon identification >4%, 1km, 10**20eV Note 2

Temperature tolerance -10C < T < 50C Conditions at Dugway

Life time 20 years

Percent of array down <5% Operating cost

Maintenance frequency <0.5 times / year Operating cost

Power per station <5 watts

Notes:

1. James W. Cronin, "Design Considerations for a Giant Surface Array," Adelaide Workshop, January 4-15, 1983
2. James W. Cronin, "Design Considerations for a Ground Array." Snowmass '94, August 1994.
3. James W. Cronin, "Segmentation and Time Resolution Required for Surface Detectors in a Giant Air Shower Array," April 25, 1994.
4. James W. Cronin, "Design Concept for a 5000 km² Air Shower Array", June 1994?

A Large Area Air Shower Detector Using Optical Fiber Readout - P. Mantch, S. Gauray, J. Ozellis

January 1995

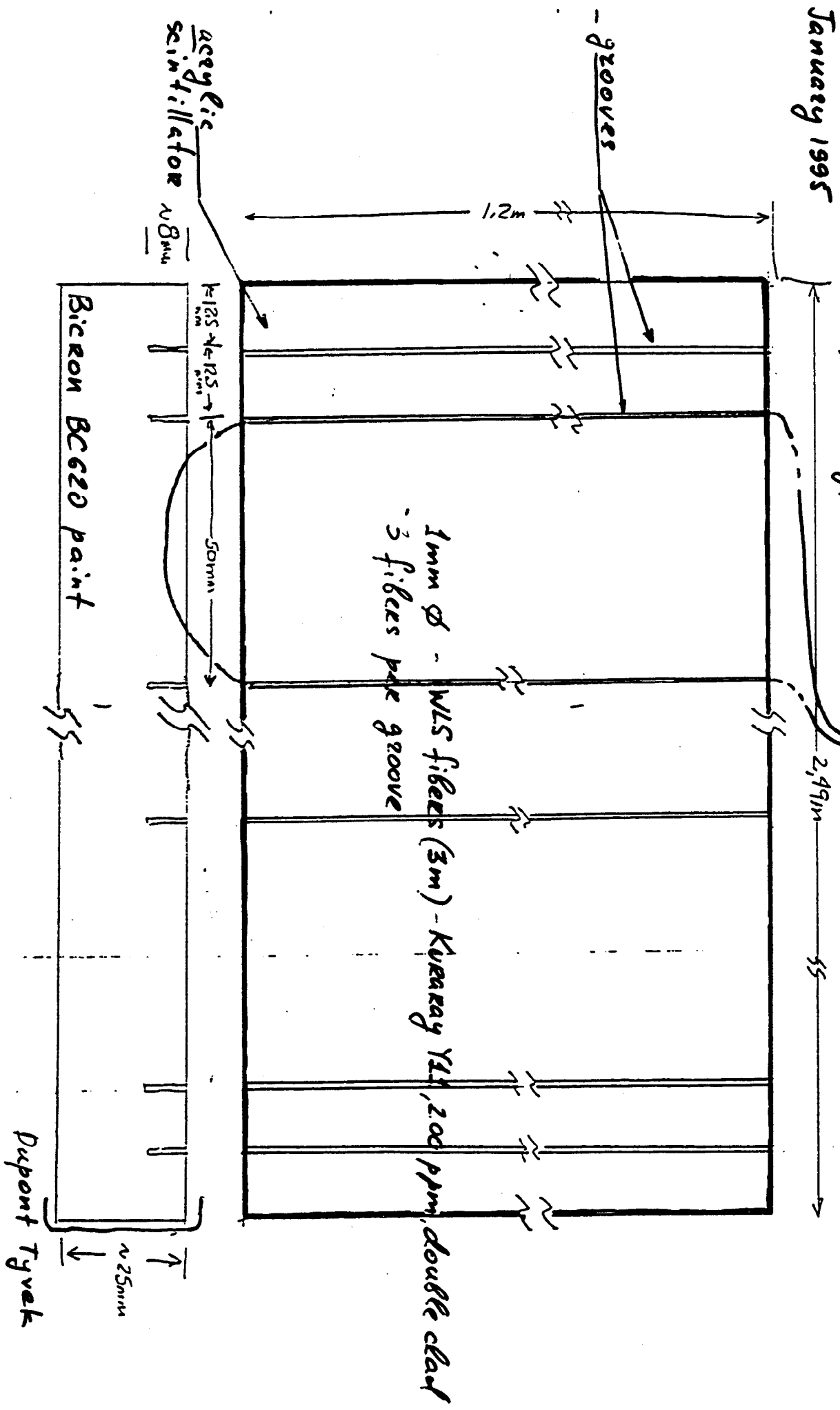


Fig. 1 TEST COUNTER DETAIL

Ampl. Spectrum of Upper 3 m² Counter (U=1450 V)

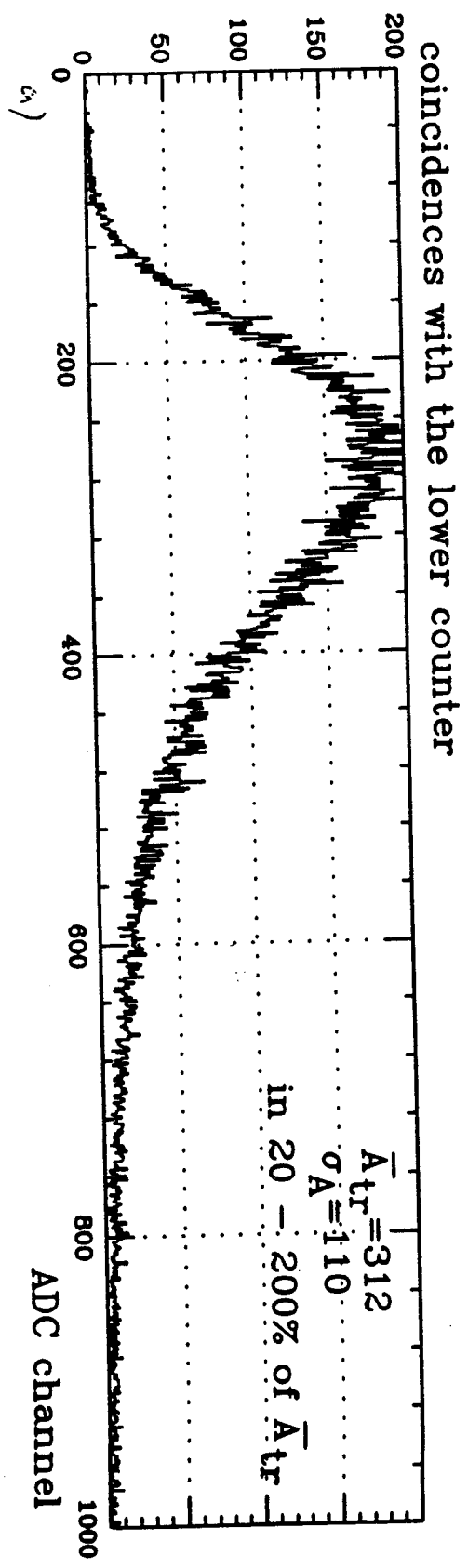
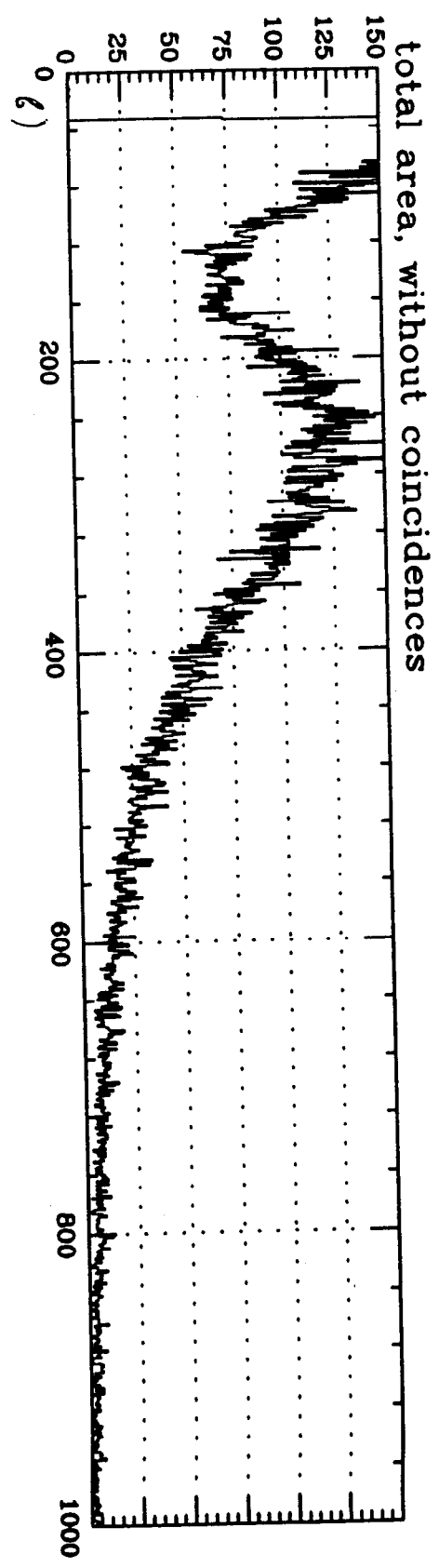
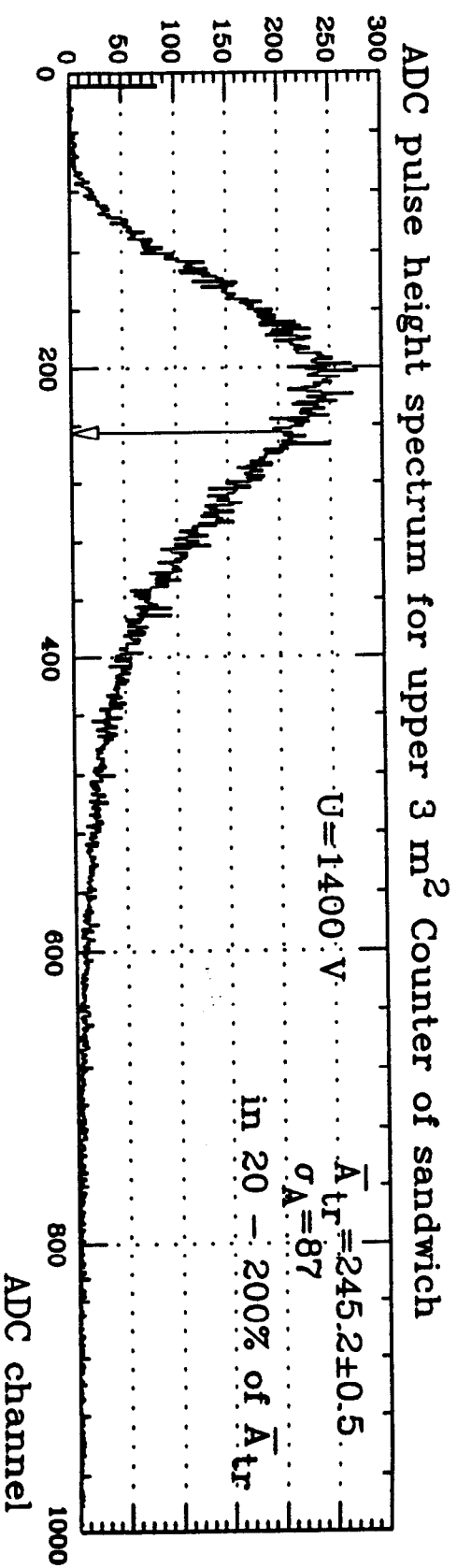
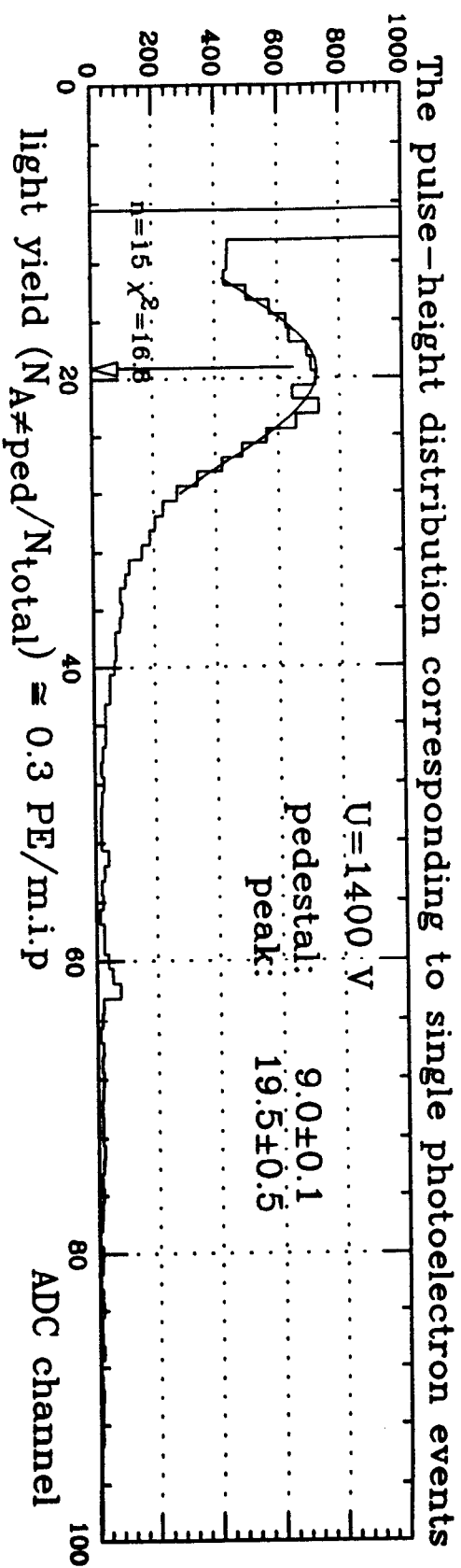


Fig. 2

Calibration of the phototube used in upper 3 m² Counter (U=1400 V)



$$N_{\text{p.e.}} = (\bar{A}_{\text{tr}} - \text{pedestal}) / (\text{peak} - \text{pedestal}) = 23 \pm 1$$

Fig. 3

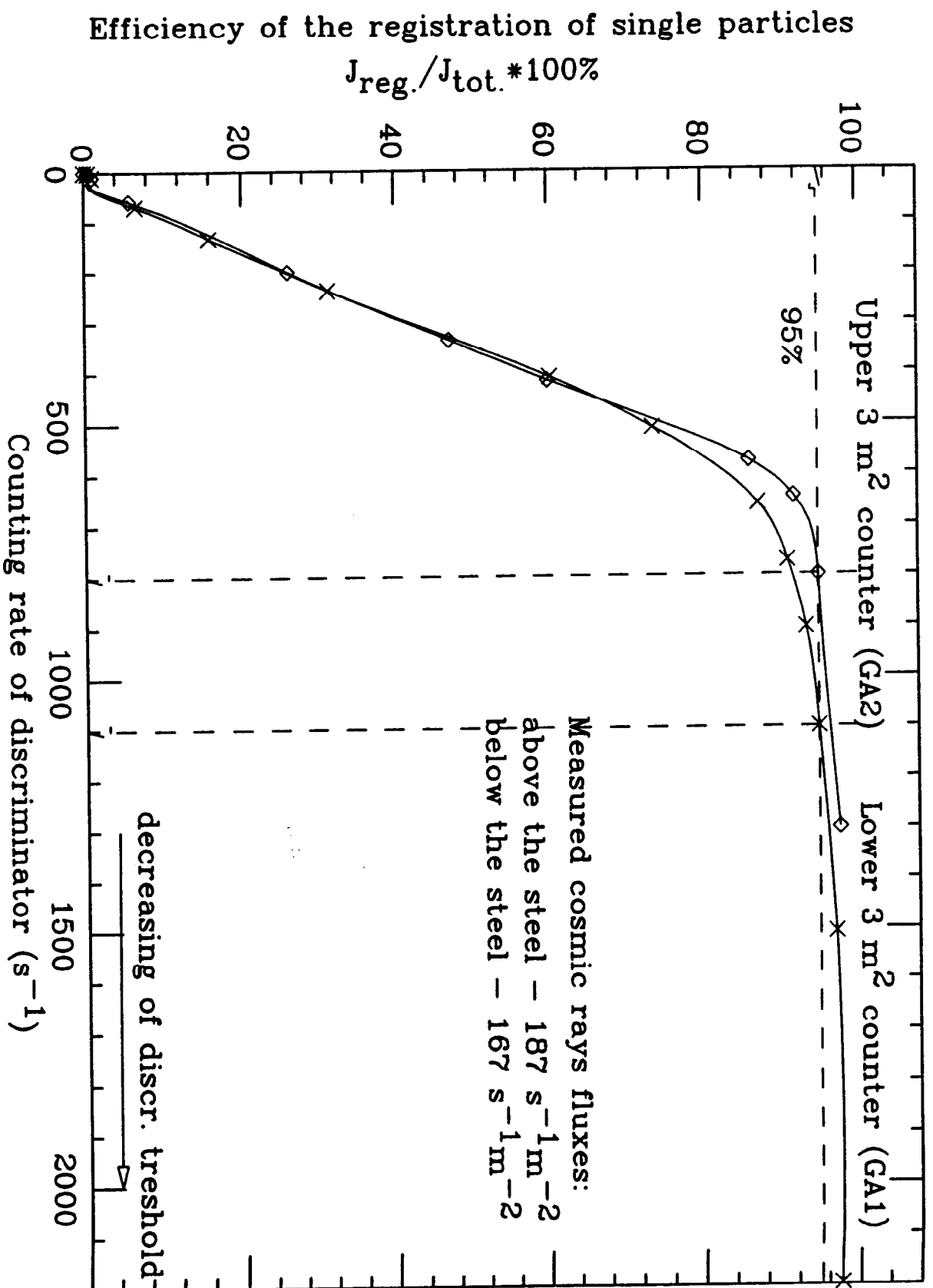
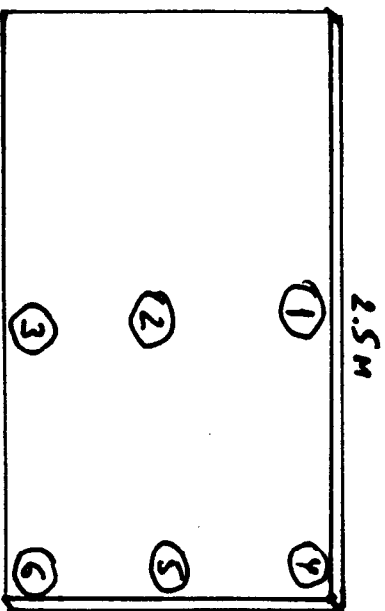


Fig. 4

Study of areal uniformity of 3 m² scintillation counters in sandwich

Red - lower counter
Green - upper counter



Lower counter:

$$\bar{A}_{\max}/\bar{A}_{\min} \sim 1.3$$

Upper counter:

$$\bar{A}_{\max}/\bar{A}_{\min} \sim 1.3$$

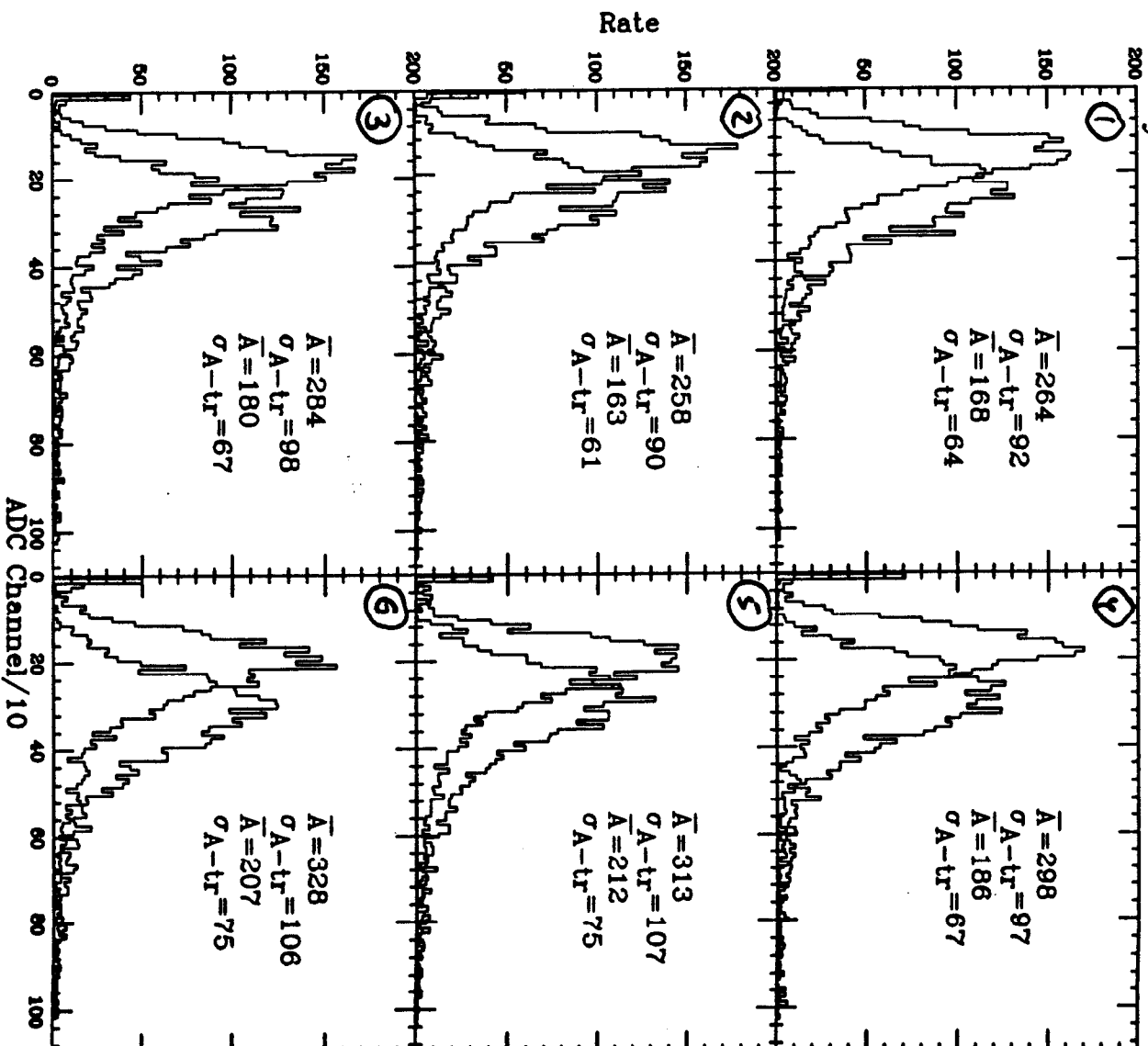
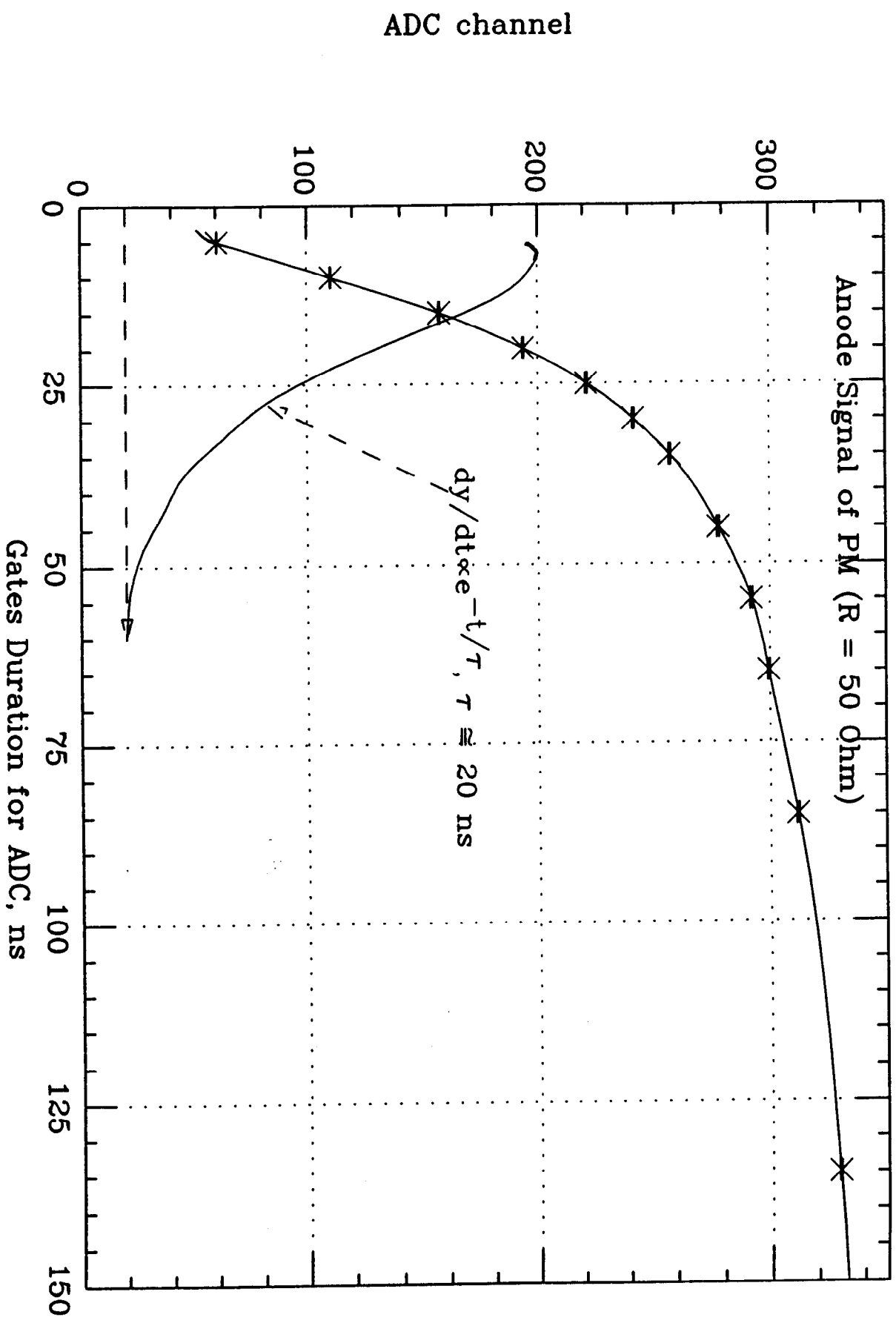


Fig. 5

Trunc. mean in pulse height distr. vs duration of gates for Charge ADC



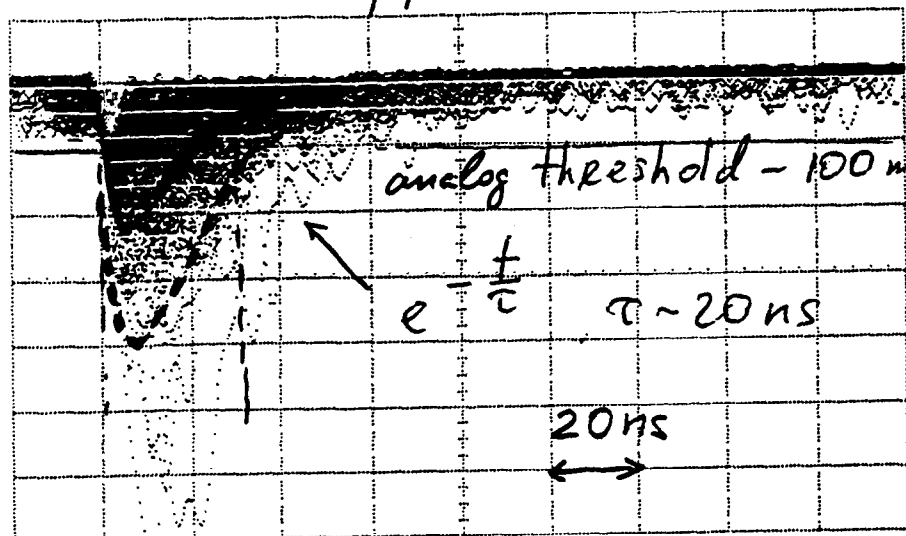
Average pulse duration on the level of 1/10 Amplitude ≈ 60 ns

Fig. 6

hp stopped

upper 3 m² counter

U = 1400 V



1 100 mV/div
offset: 300.0 mV
1.000:1 50% dc

analog threshold - 100 mV, $f = 800 \text{ s}^{-1}$, 55% reg

$e^{-t/\tau}$ $\tau \sim 20 \text{ ns}$

20 ns

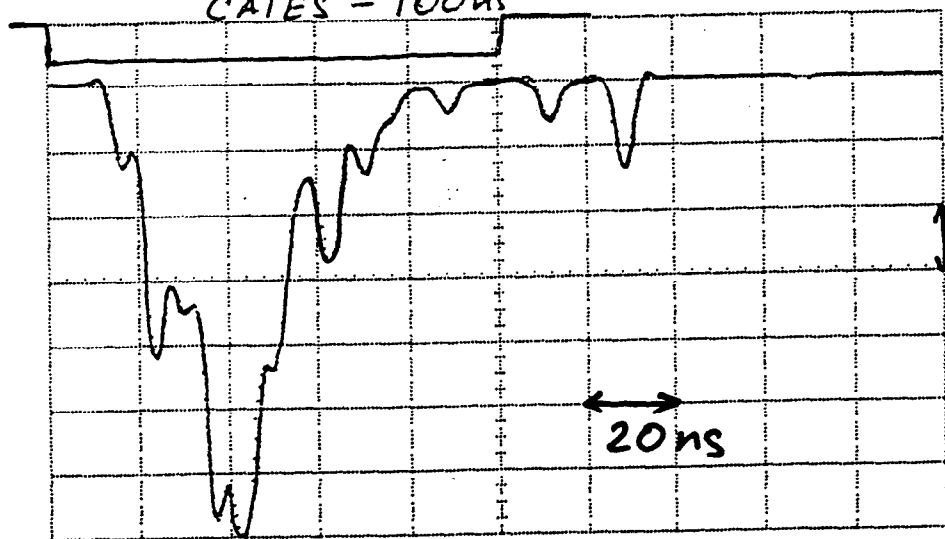
-135.200 ns -35.200 ns 64.800 ns
20.0 ns/div

	current	minimum	maximum	average
Vamp(1)	109.375 mV	64.375 mV	667.500 mV	<u>204.609 mV</u>

EXT \overline{V} -62.50 mV

hp stopped

CATES - 100 ns



1 50.0 mV/div
offset: 150.0 mV
1.000:1 50% dc

50 mV

20 ns

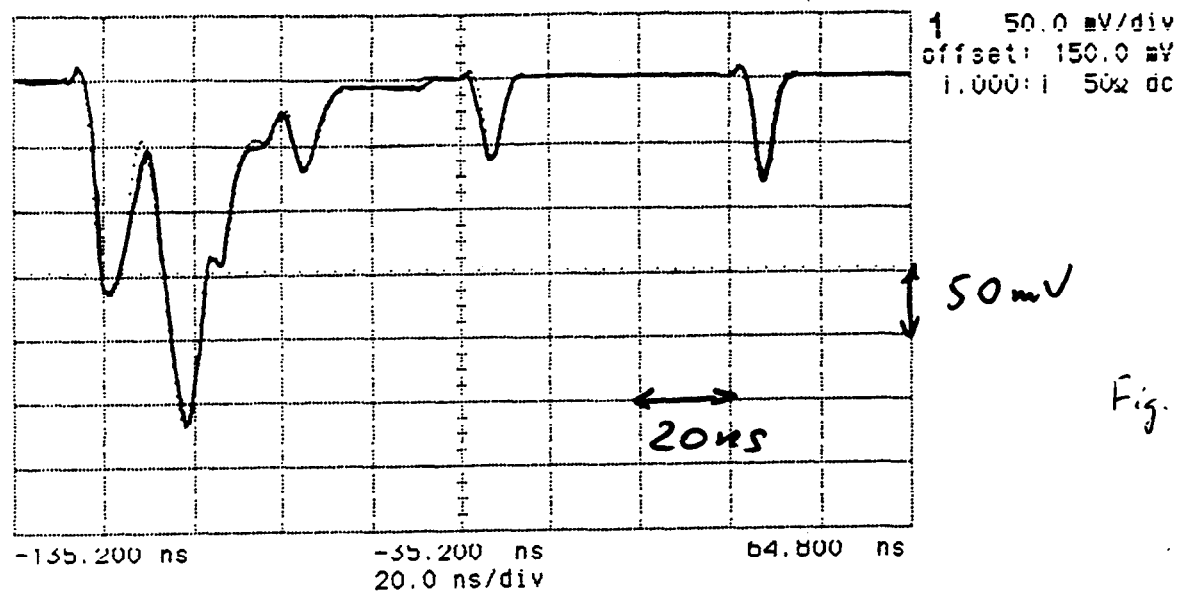
-135.200 ns -35.200 ns 64.800 ns
20.0 ns/div

	current	minimum	maximum	average
Vamp(1)	clipped	-----	-----	-----

EXT \overline{V} -62.50 mV

X

As stopped

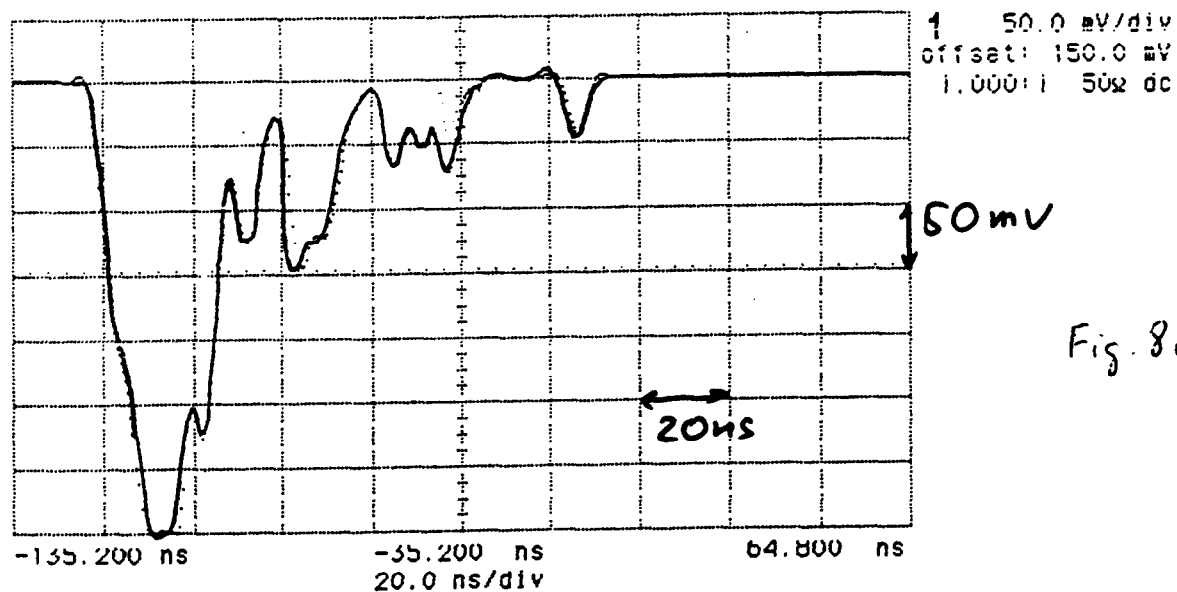


	current	minimum	maximum	average
Vamp(1)	270.313mV	270.313mV	270.313mV	270.313mV

EXT \overline{V} -62.50 mV

Fig. 8b

As stopped



	current	minimum	maximum	average
Vamp(1)	clipped	-----	-----	-----

EXT \overline{V} -62.50 mV

Fig. 8c

Distribution of time intervals between 2 signals of PM's discriminator

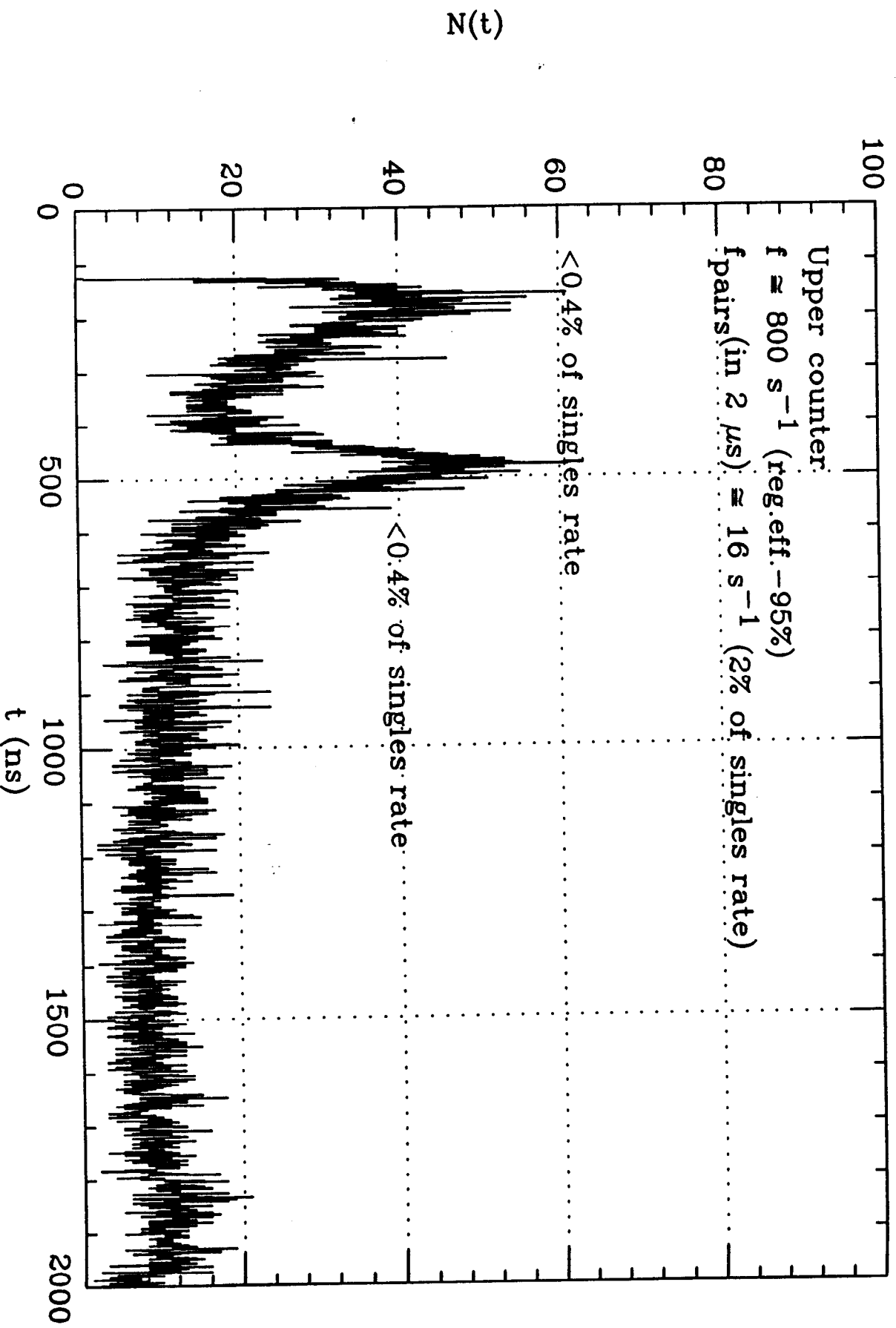
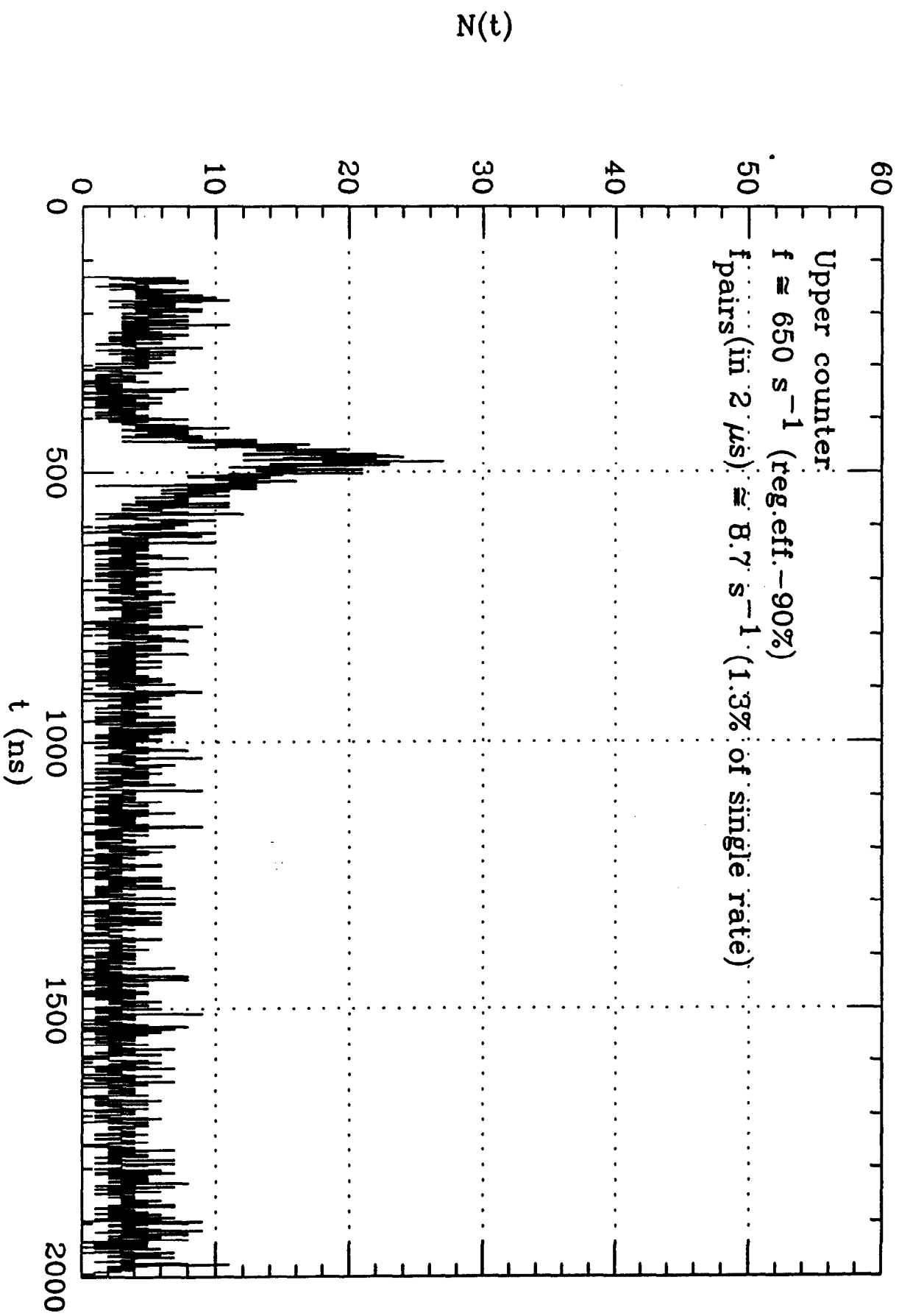


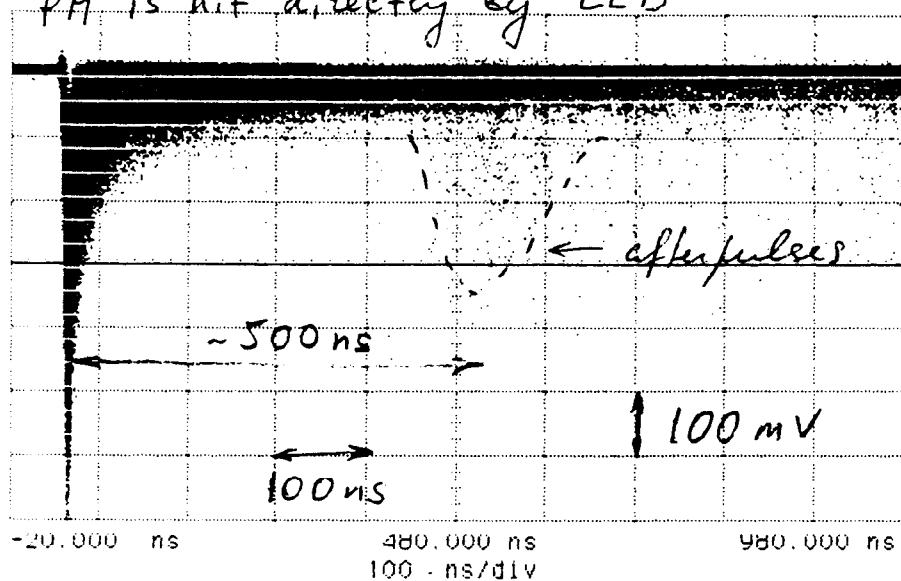
Fig. 3

Distribution of time intervals between 2 signals of PM's discriminator



50 running

PM is hit directly by LED



1 100 mV/div
offset: 300.0 mV
1.000:1 50Ω dc

2 500 mV/div
offset: 0.000 V
1.000:1 50Ω dc

Vamp(f)	current			
	minimum	maximum	average	
	350.000mV	100.000mV	703.125mV	330.643mV

PM EMI-9502KB 38MM

Fig 96

Distribution of time intervals between 2 sequential signals in sandwich

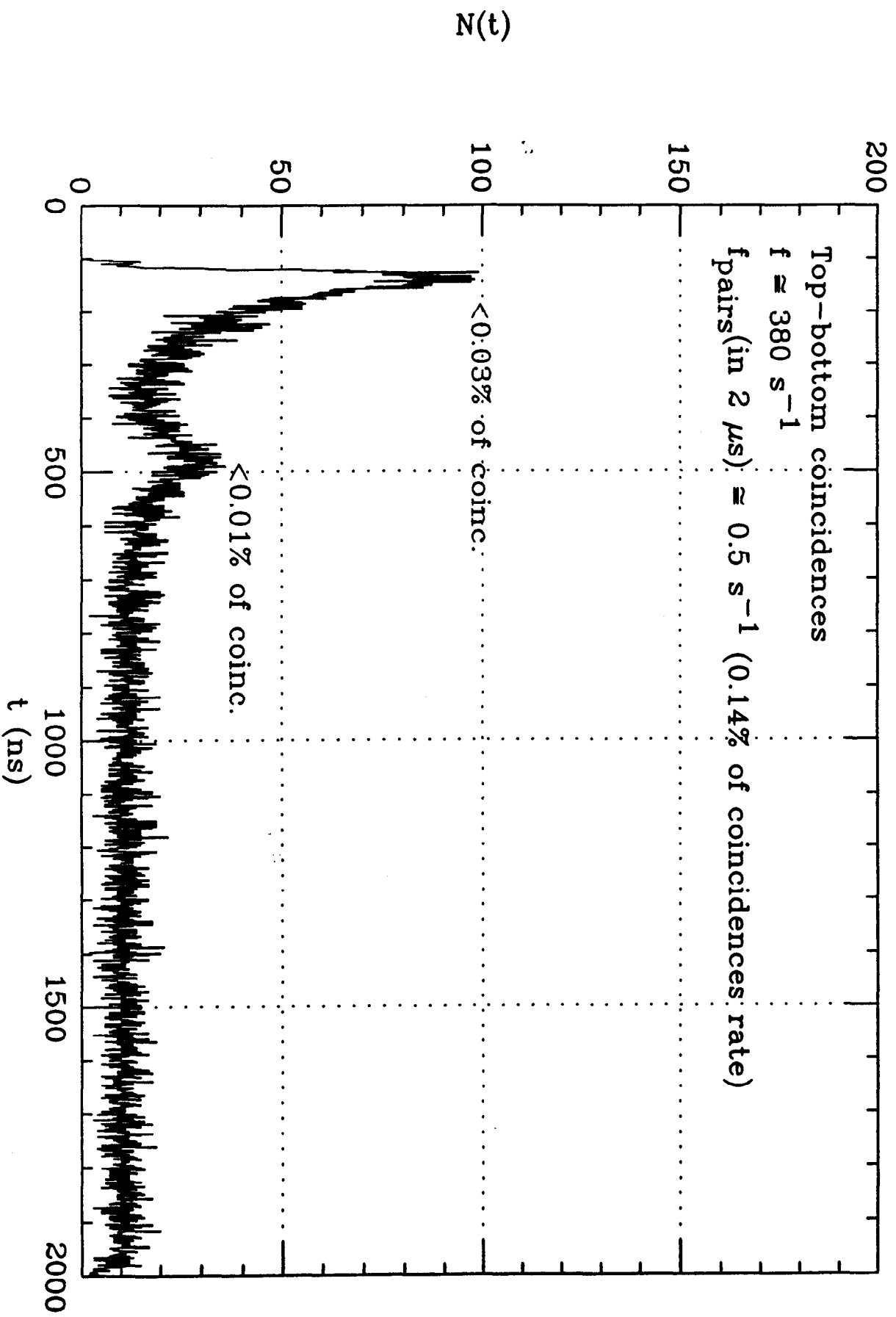


Fig. 10

Time resolution of 3 m² scintillation counter in Sandwich

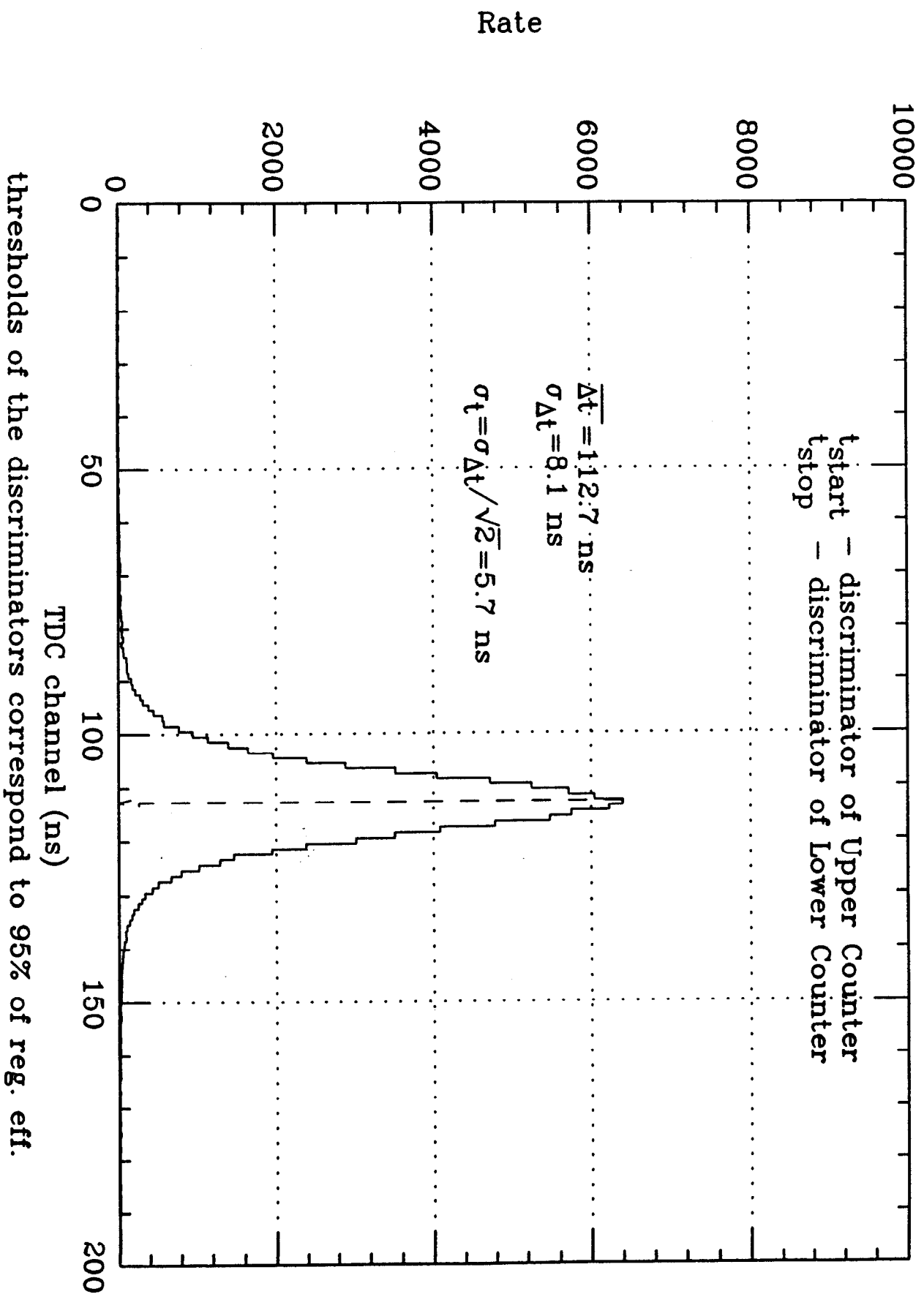


Fig. 11

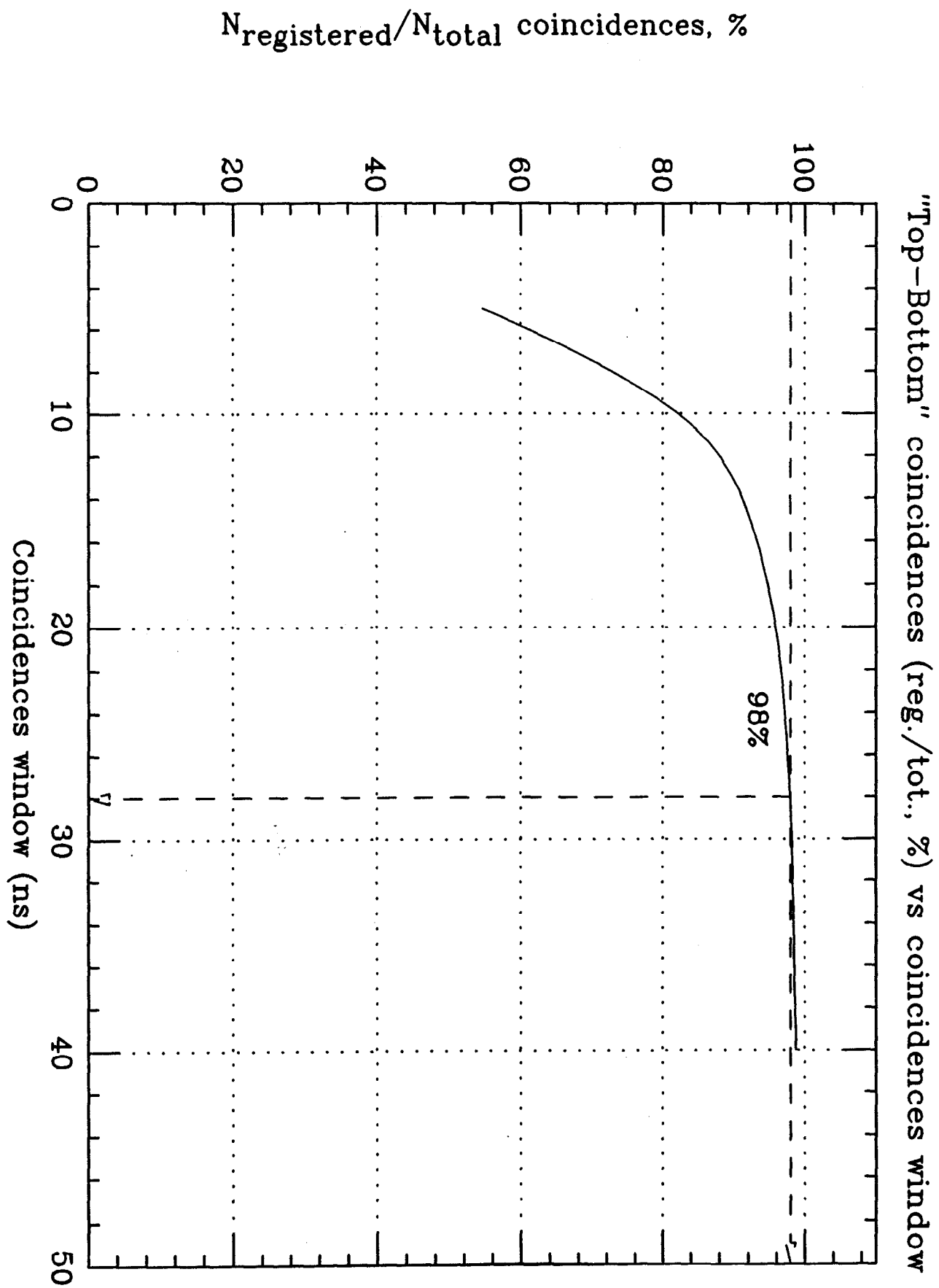
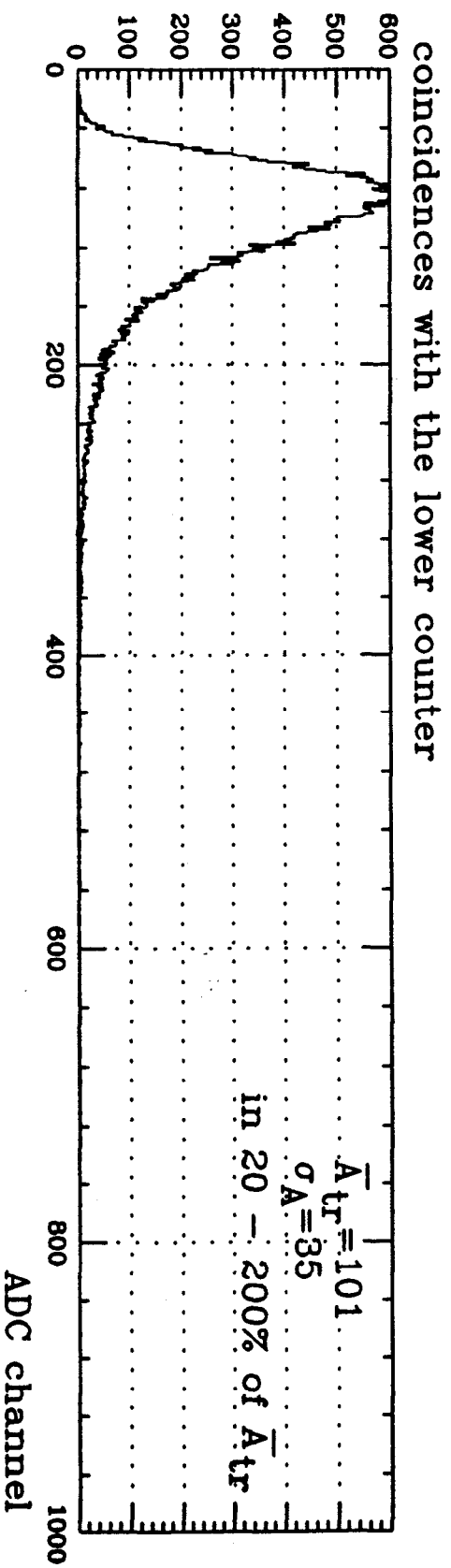
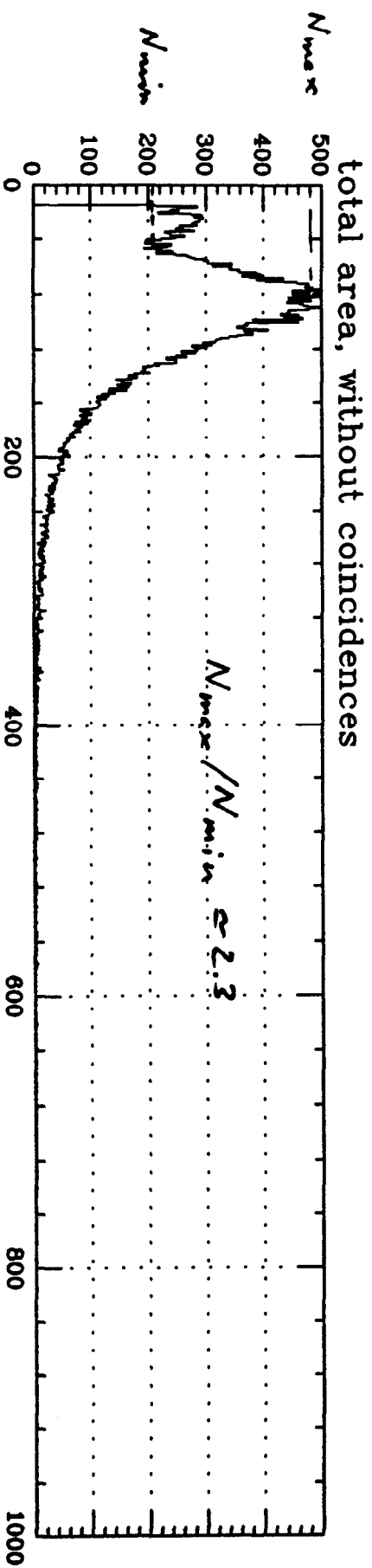
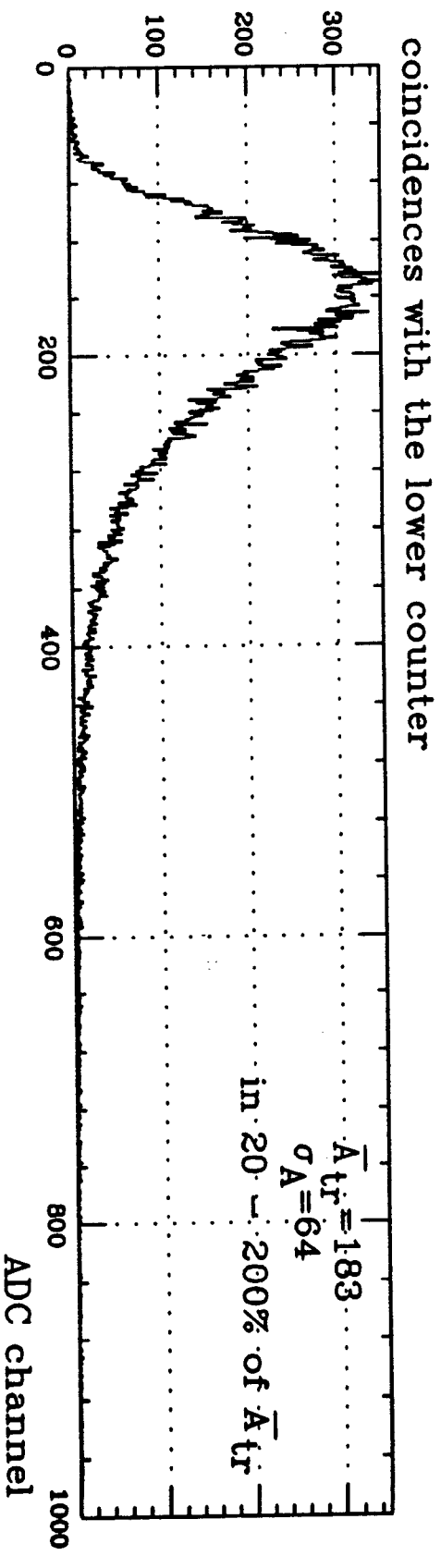
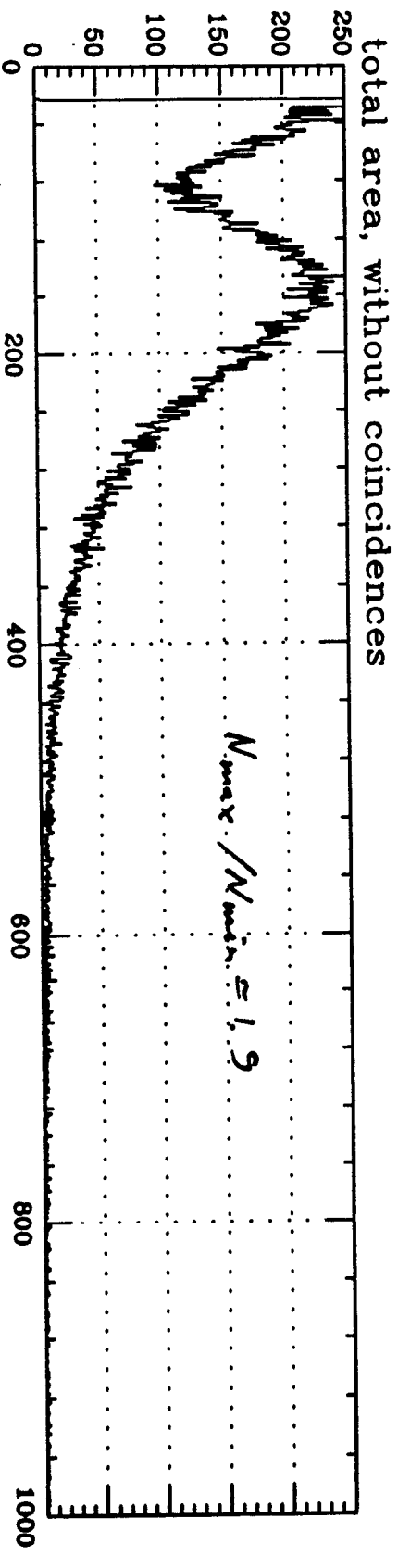


Fig. 12

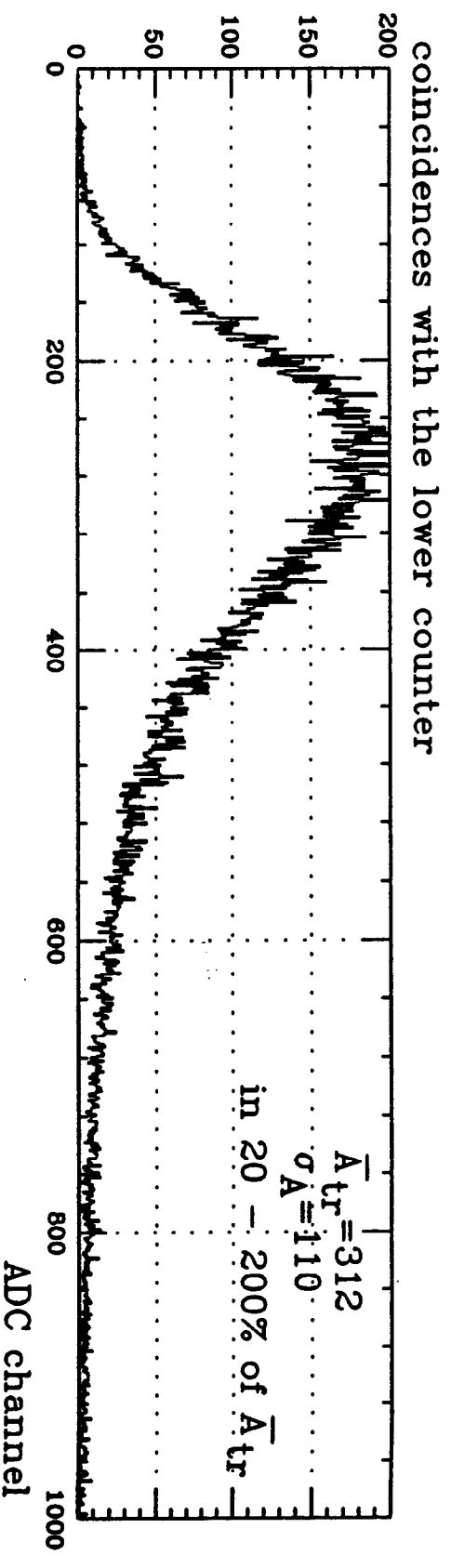
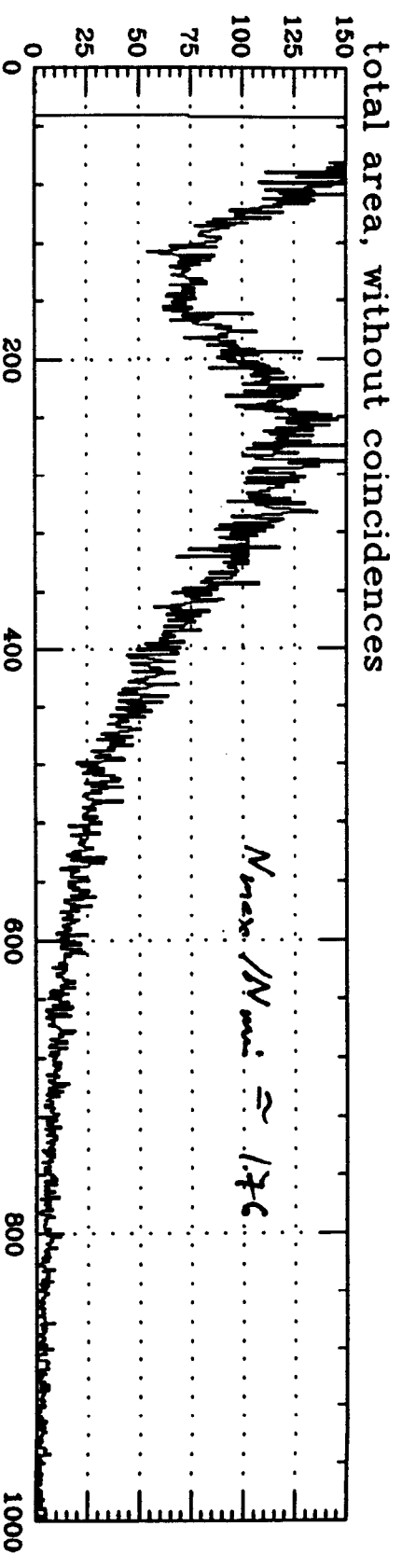
Ampl. Spectrum of Upper 3 m² Counter (U=1200 V)



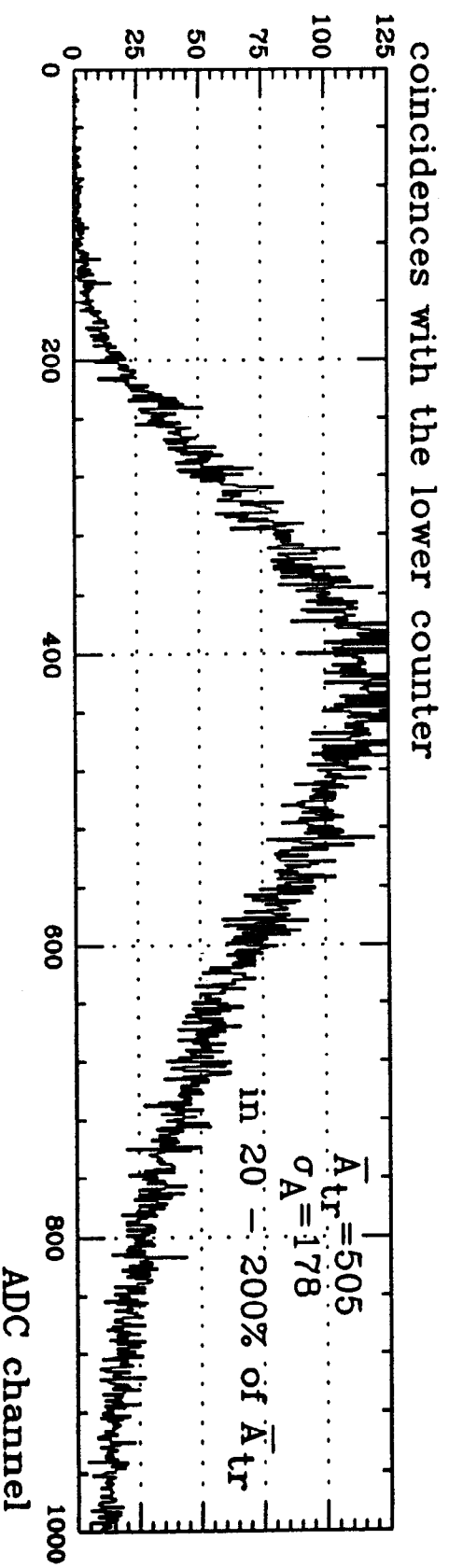
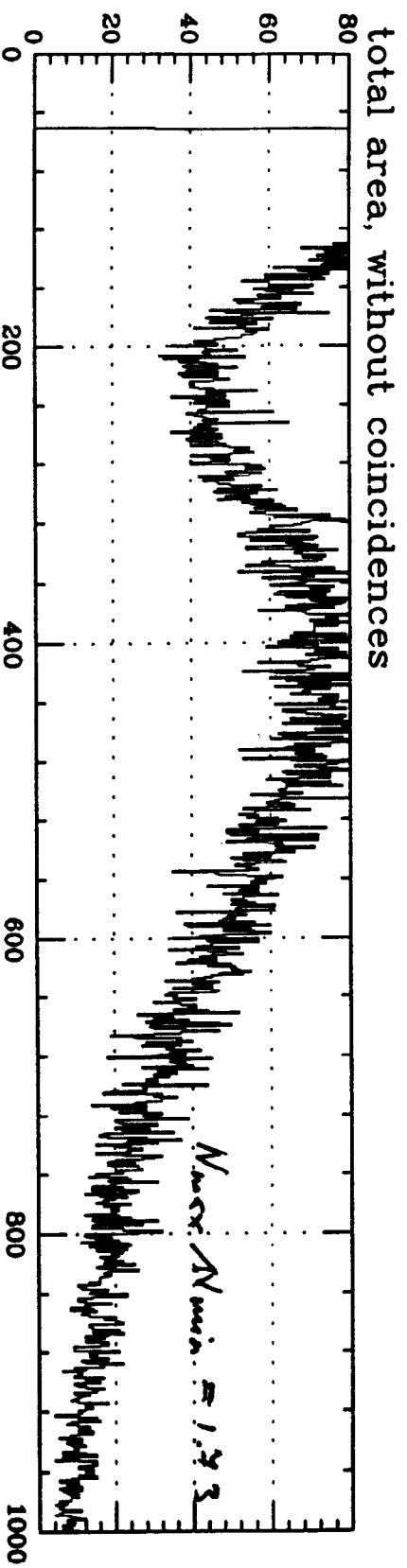
Ampl. Spectrum of Upper 3 m² Counter (U=1300 V)



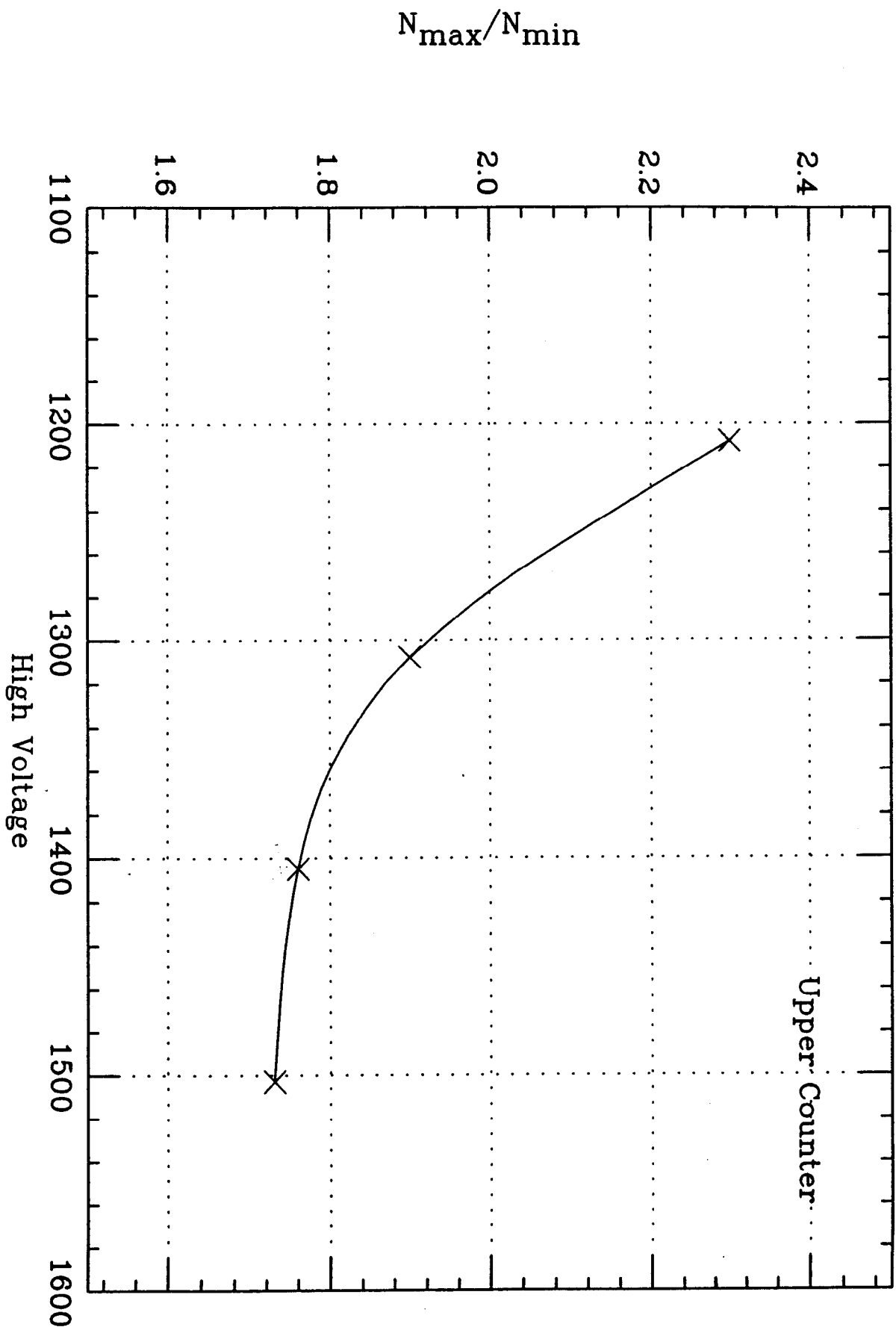
Ampl. Spectrum of Upper 3 m² Counter (U=1400 V)



Ampl. Spectrum of Upper 3 m² Counter (U=1500 V)



Depth of minimum between signal peak and noise in Ampl. Spectrum vs HV



Truncated Mean in Ampl. Spectrum vs HV

